JOURNAL OF SPACECRAFT AND ROCKETS
Vol. 29, No. 5, September–October 1992

Three-Dimensional Finite Element Analysis of Crack-Defect Interaction

C. T. Liu*
Phillips Laboratory, Edwards Air Force Base, California 93523

A three-dimensional elastic analysis of crack-defect interaction was conducted using finite element methods. The defect was modeled by setting the Young's modulus of the defect material equal to 0.1 psi. The effects of the size and the location of the defect on the magnitude and the distribution of the mode 1 stress intensity factor along the crack front and the stress distribution near the crack tip are evaluated and the results are discussed.

I. Introduction

AN important engineering problem in solid rocket motor structural design involves evaluating structural strength and reliability. It is well known that structural strength may be degraded due to the presence of imperfections in the solid propellant. These imperfections may be produced during manufacturing of the rocket motor. In analyzing the strength of a solid propellant, the localized imperfection may be idealized as a crack in the material. Besides the idealized cracks, large cracks can also develop in the propellant during storage, firing, etc. When cracks occur, whether resulting from the manufacturing process or from the service loads, the stress near the crack tip in a stressed body will be redistributed. Depending on the magnitude of the local stress and the local material strength, various intensities of damage, or defects, can develop near the crack tip region. And, depending on the severity of the defect, the crack growth behavior can be significantly affected. Therefore, to obtain a fundamental understanding of crack growth behavior in solid propellants, the interaction between the crack and the defects needs to be determined.

During the past years, a considerable amount of work has been done in studying crack interaction[1,2] and crack-defect interaction.[3-5] In those studies, the effects of through-thickness microcracks and defects on the stress intensity factors can be increased or decreased. It is believed that the fluctuation in the stress intensity factor is a contributing factor to the fluctuation in crack growth rate that is observed during crack propagation testing. Experimental observation also reveals that voids of different sizes can develop either inside or on the surface of the specimen. Therefore, to obtain a fundamental understanding of how a nonthrough-thickness void will affect the stress intensity factor at the main crack tip and how the stress will transfer in the specimen, a three-dimensional analysis should be conducted.

In this study, a three-dimensional elastic finite element computer code, known as TEXGAP-3D, was used to determine the stress intensity factor at the crack tip as well as the stress distribution in the specimen. The specimen was 8.0 in. long, 2.0 in. wide, and 0.6 in. thick. A 1.5-in. crack, which was parallel to the longest side of the specimen and perpendicular to the loading direction, was cut at the center of the specimen. The geometry of the centrally cracked specimen with a defect near the crack tip is shown in Fig. 1. In the finite element analysis, a constant displacement of 0.25 in., which was normal to the horizontal centerline of the crack, was applied at the boundary of the specimen. The defect was modeled by setting its modulus equal to 0.1 psi. The modulus of the undamaged material was equal to 500 psi. A constant Poisson's ratio of 0.4999 was used in the analysis. For comparison purposes, a 0.2-in.-thick thin specimen with a through-thickness defect of the same size and location as the defect in the thick specimen was also analyzed. The results of the finite element analysis were analyzed and the effect of defect characteristics on the value of the stress intensity factor as well as the stress distribution near the crack tip were discussed. In addition, the effects of crack-defect interaction on crack growth behavior were also discussed.

II. Finite Element Analysis

In this study, a three-dimensional elastic finite element computer code, known as TEXGAP-3D, was used to determine the stress intensity factor at the crack tip as well as the stress distribution in the specimen. The TEXGAP-3D computer code contains conventional and reformulated elements and can be used to analyze both compressible and incompressible materials. It also contains conventional crack elements derived from a hybrid displacement model. These crack elements, originally developed by Kathiresan and Atluri,[6] were developed for modeling compressible materials. Therefore, they cannot be used to solve problems involving incompressible materials. However, for nearly incompressible materials, it has been determined that the finite element solution and the theoretical solution differ by 2.7% for a Poisson's ratio equal to 0.4999.[7] In addition, the finite element solution is also compared with the photoelastic solution for the cracked biaxial specimen obtained by Theiss.[8] It has been found that these two solutions differ by 2.28%. However, it should be pointed out that the photoelastic solution contains approximately 5% experimental scatter.

In this study, the specimen, shown in Fig. 1, was divided into six 0.1-in. layers in the thickness direction. Because of symmetry conditions, only 1/8 of the specimen was modeled as shown in Fig. 2. The finite element model consisted of three 0.1-in.-thick layers, denoted as outside layer, middle layer, and inside layer. The defect elements were elements 13 and 14

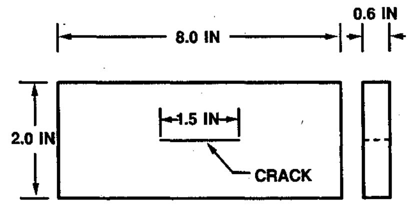

Fig. 1 Specimen geometry.

Presented as Paper 90-0927 at the AIAA/ASME/ASCE/AHS/ASC Structures, Structural Dynamics, and Materials Conference, Long Beach, CA, April 2–4, 1990; received March 21, 1991; revision received April 19, 1992; accepted for publication April 20, 1992.

*Project Manager. Member AIAA.

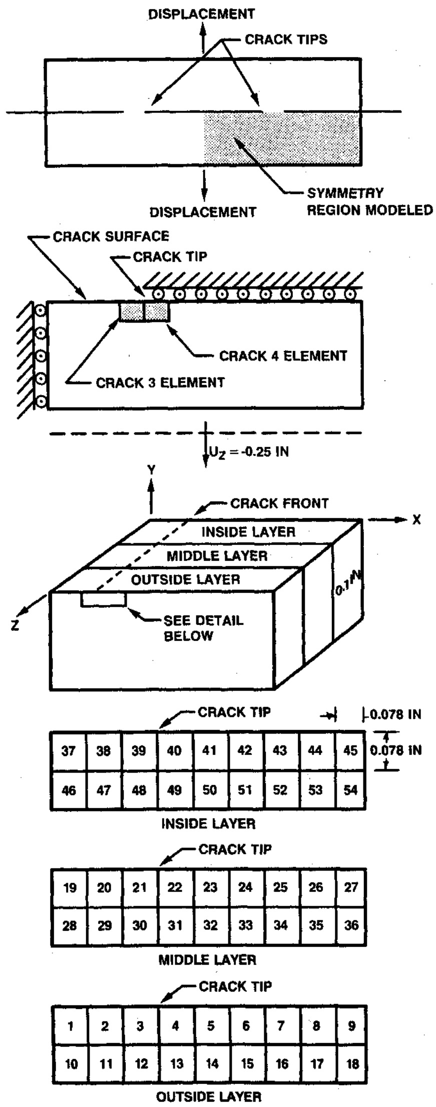

Fig. 2 Finite element model.

in the outside layer, 31 and 32 in the middle layer, and 49 and 50 in the inside layer. In the finite element model, SLOPE boundary conditions (the SLOPE boundary condition produces the same effect as the rollers shown schematically in Fig. 2b were applied on appropriate surfaces as indicated in Fig. 2b as well as on the back face of the model as viewed in Fig. 2b. A frictionless (shear-free) displacement boundary condition ($U = -0.25$ in.) was imposed on the lower boundary. The right boundary and the crack surface itself were modeled as free surfaces. Two hybrid crack elements, denoted as CRACK 3 and CRACK 4, were used at the crack tip to model the quadrant containing the free surface and the quadrant without a free surface, respectively. As mentioned before, these crack elements are not reformulated for incompressibility but they provide a reasonably accurate solution.

In the analysis, a Poisson's ratio of 0.4999 and a modulus of 500 psi were used for the undamaged material, and the defect was modeled by setting the modulus of the defect element equal to 0.1 psi. It should be pointed out that since only 1/8 of the specimen was modeled, there were actually eight defects in the specimen and they were located symmetrically with respect to the vertical and the horizontal planes of symmetry of the specimen. In the finite element analysis, for comparison purposes, a 0.2-in.-thick thin specimen with a through-thickness defect of the same size and location as the defect in the thick specimen was also analyzed. The results of the finite element analysis are discussed in the following paragraph.

III. Results and Discussion

A summary of the calculated mode I stress intensity factor K_I at the crack tip is shown in Table 1. From Table 1, it is seen that, for the baseline case in which there is no defect, the value of K_I varies along the crack front. The largest value (175.79 psi $\sqrt{\text{in.}}$) occurs at the center of the specimen whereas the smallest value (164.12 psi $\sqrt{\text{in.}}$) occurs near the surface of the specimen. It is interesting to note that the average value of K_I in the thick specimen, with a thickness equal to 0.6 in., is 171.08 psi $\sqrt{\text{in.}}$, whereas the value of K_I in the thin specimen, with a thickness equal to 0.2 in., is 170.25 psi $\sqrt{\text{in.}}$ This indicates that, on the first approximation, the average value of K_I is not affected by the two specimen thicknesses considered in this study. This finite element result is consistent with the experimental result obtained by Post et al.[9] By using the photoelastic method, it is found that the value of K_I in a 0.5-in.-thick specimen is approximately equal to that in a 0.25-in.-thick specimen. This indicates that the photoelastic method tends to obscure the three-dimensional nature of the stress field in a thick specimen.

From Table 1, we see that, by comparing with the baseline case, the presence of a through-thickness defect in the vicinity of the crack induces a higher magnitude and different distribution of K_I through the thickness of the specimen. For this case, the values of K_I in the inside, middle, and outside layers are 182.48 psi $\sqrt{\text{in.}}$, 184.69 psi $\sqrt{\text{in.}}$, and 182.66 psi $\sqrt{\text{in.}}$, respec-

Table 1 Summary of results of crack-defect interaction analysis

Case no.	Defect element	Inside layer K_I, psi $\sqrt{\text{in.}}$	Middle layer K_I, psi $\sqrt{\text{in.}}$	Outside layer K_I, psi $\sqrt{\text{in.}}$	Thin specimen K_I, psi $\sqrt{\text{in.}}$
1	None	175.79	173.33	164.12	170.25
2	13, 14	183.00	183.29	161.49	
3	13, 14, 31, 32	195.19	172.61	165.85	
4	13, 14, 31, 32 49, 50	182.48	184.69	182.66	185.40
5	49, 50	169.49	181.00	171.88	
6	49, 50, 31, 32	178.74	174.77	178.82	
7	31, 32	182.44	162.86	169.55	
8	31, 32 $E = 0.001$ psi	183.79	159.26	170.04	

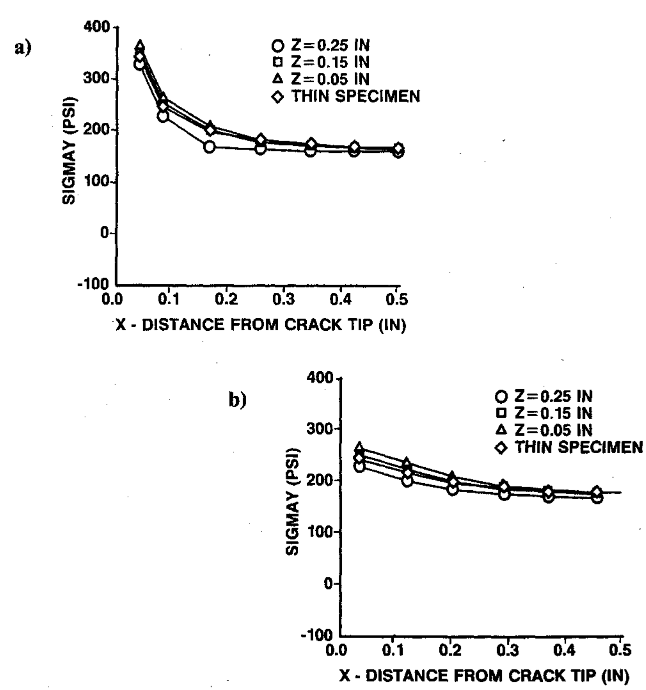

Fig. 3 Normal stress distribution (case 1): a) along crack plane; and b) along defect plane.

tively. Similar to the baseline case, the average value of K_I, which is equal to 183.28 psi $\sqrt{\text{in.}}$, in the thick specimen is approximately equal to that in the thin specimen. Referring back to Table 1, we note that, by comparing with the baseline case, the presence of a defect in a given layer will reduce the value of K_I in that layer and increase the values of K_I in the other layers. However, when there are defects present in two of the layers, whether the values of K_I increase or decrease in the defect layers will depend on the location of the defect. But, in general, the value of K_I will increase in the layer containing no defects. For example, an 11% increase in the value of K_I in the inside layer occurs when a defect is present in the middle and the outside layers, and an 8.96% increase in the value of K_I in the outside layer occurs when a defect is present in the middle and the inside layers. Referring back to Table 1, we note that the magnitude and the distribution of K_I along the crack front depend on the location and the size of the defect. Because of the complex interaction between the crack and the defect, there is no consistent trend as far as the effect of the defect on the magnitude and distribution of K_I is concerned.

As already discussed, the presence of a through-thickness defect or the presence of defects in both the inside and the middle layers induces a relatively uniform distribution of K_I along the crack front. Since the crack growth behavior is controlled by the local stress, or the stress intensity factor K_I, the relatively uniform distribution of K_I along the crack front will result in a relatively uniform crack growth front. For the

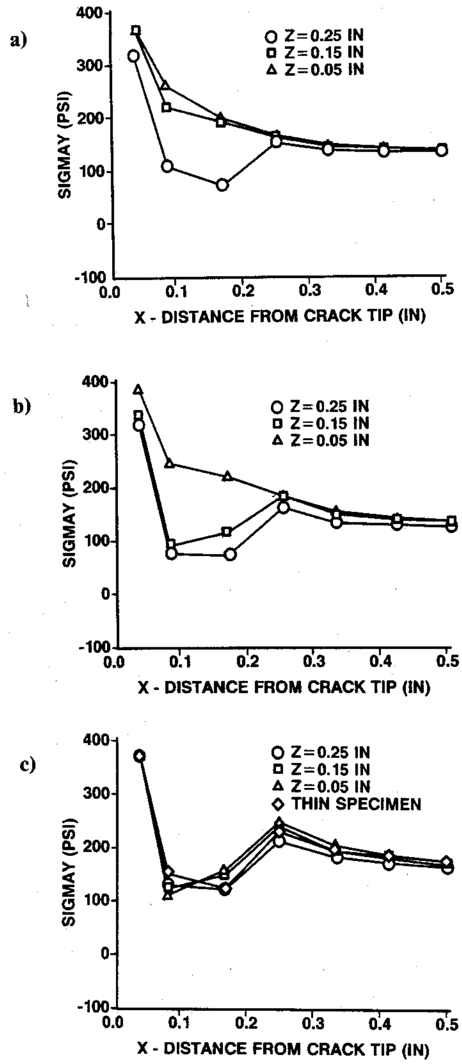

Fig. 4 Normal stress distribution along crack plane: a) case 2; b) case 3; and c) case 4.

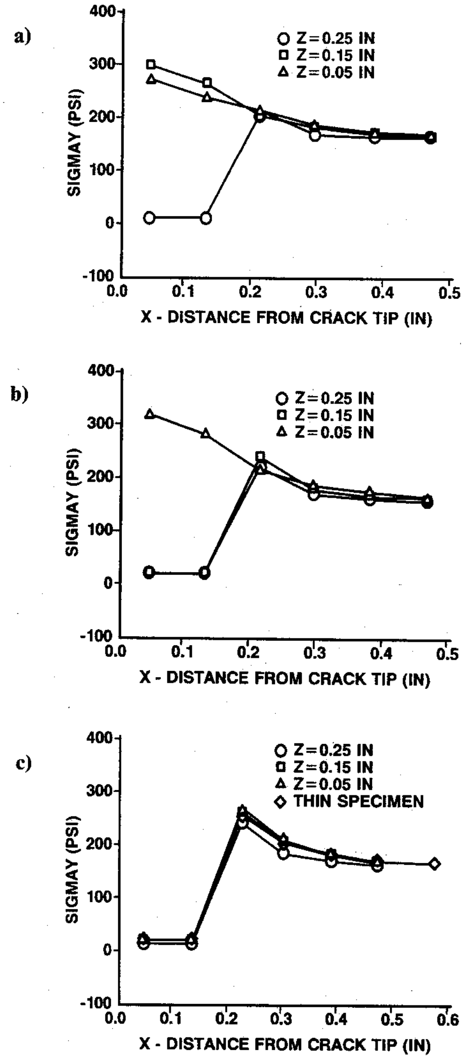

Fig. 5 Normal stress distribution along defect plane: a) case 2; b) case 3; and c) case 4.

other nonthrough-thickness defect cases, the irregular distribution of K_I along the crack front is one of the contributing factors to the irregular crack growth in the thickness direction of the specimen. The relatively straight crack growth front has been observed and reported by Post et al.[10] in their study of crack growth behavior in a composite solid propellant. Based on experimental findings, Post et al. pointed out that a large number of voids developed in the failure process zone which is in the immediate vicinity of the crack tip. Consequently, the transverse constraint is minimized, resulting in a relatively straight crack growth front. The present finite element analysis indicates that the presence of a large interior defect or a through-thickness defect near the crack tip will also minimize the transverse constraint.

This discussion is centered on the effect of defects on the magnitude and distribution of K_I along the crack front. To see how the defect affects the stress distribution in the specimen, the results of the finite element analysis were analyzed. A detailed discussion on the normal stress distribution, which is thought to be most interesting, in the presence of a defect is presented in the following paragraphs.

Plots of the normal stress σ_y along the crack plane ($y = 0$ in.) and the defect plane ($y = 0.0118$ in.) for the baseline case (refer to Table 1, case 1) are shown in Figs. 3a and 3b. For comparison purposes, the distribution of σ_y in the thin specimen, which has a thickness equal to 0.2 in., is also shown in Figs. 3a and 3b. From these figures we see that the magnitude of σ_y

increases as the value of Z decreases. In other words, the stress is higher in the interior of the specimen. A close examination of Figs. 3a and 3b reveals that the distributions of σ_y in the thin specimen are very close to the distributions of the thickness-averaged value of σ_y in the thick specimen. This phenomenon is similar to that observed earlier when the effect of specimen thickness on the value of the stress intensity factor was investigated.

Plots of the distribution of σ_y along the crack plane and the defect plane for cases 2–4 are shown in Figs. 4 and 5. By comparing Fig. 3a with Fig. 4, we see that, within the same layer, the presence of a defect can significantly reduce the magnitude of σ_y in the element directly above the defect element. This indicates that the presence of a defect produces a "shielding" effect on the element directly above the defect element. However, the stresses in the layers which do not contain a defect are higher than those in the baseline case, especially near the crack tip region. When the distance in the x direction is increased, the values of σ_y decrease and will eventually equal the value of σ_y in the baseline case. The distance x at which the values of σ_y in cases 2–4 are equal to those in the baseline case defines the boundary of the defect-affected zone. According to Figs. 3–5, for a given length and width of the defect, the size of the defect-affected zone in the crack plane increases with increasing thickness of the defect. For example, the defect-affected zone size is approximately 0.39 in. for case 2 and 0.45 in. for case 3.

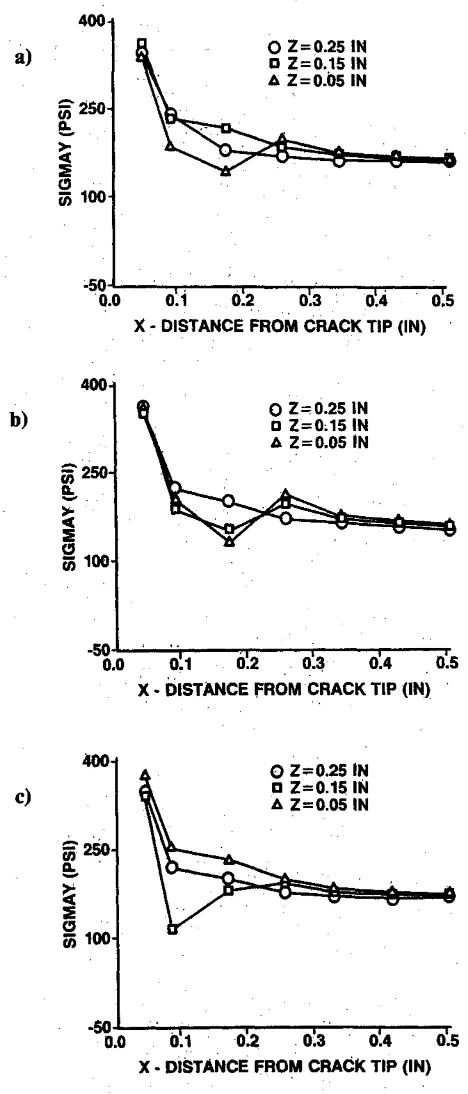

Fig. 6 Normal stress distribution along crack plane: a) case 5; b) case 6; and c) case 7.

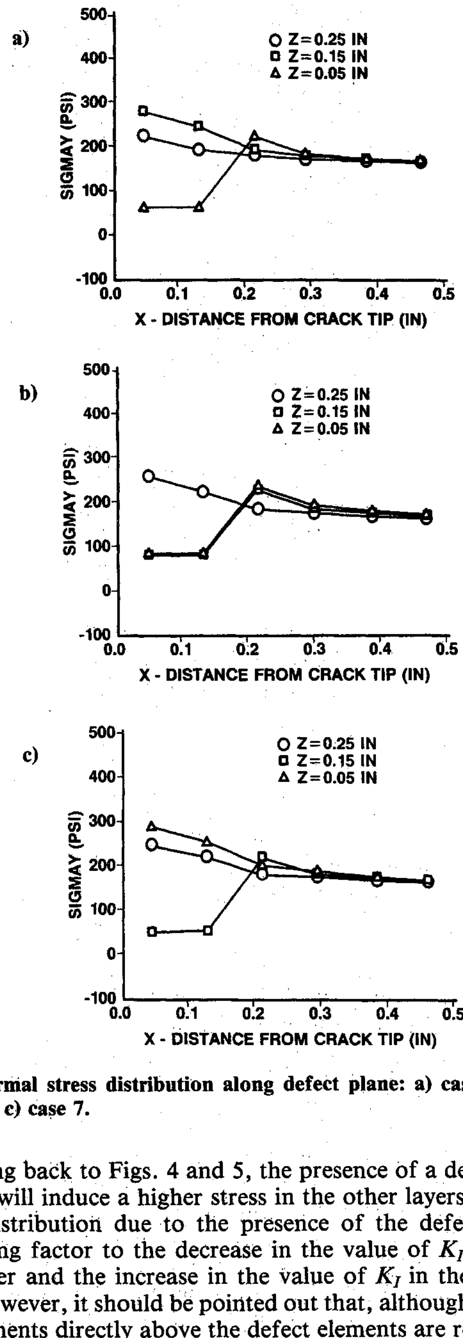

Fig. 7 Normal stress distribution along defect plane: a) case 5; b) case 6; and c) case 7.

Referring back to Figs. 4 and 5, the presence of a defect in one layer will induce a higher stress in the other layers. This stress redistribution due to the presence of the defect is a contributing factor to the decrease in the value of K_I in the defect layer and the increase in the value of K_I in the other layers. However, it should be pointed out that, although the σ_y in the elements directly above the defect elements are reduced when the defect is a through-thickness defect as in case 4, the interaction between the crack and the defect produces higher values of K_I along the crack front.

Plots of the distributions of σ_y along the crack plane and the defect plane for cases 5–7 are shown in Figs. 6 and 7. By comparing these figures with Figs. 4 and 5, we note that the conclusions drawn for cases 2–4 apply equally well to cases 5–7.

Referring back to Figs. 5 and 7, it is interesting to note that the stress in the defect elements for cases 5–7 is much higher than that in the defect elements for cases 2–4. This implies that, for the modulus (0.1 psi) used for the defect element, the higher stress is probably due to the higher constraint imposed on the defect element in the interior of the specimen. To see how the modulus of the defect element changes the stress either inside the defect element or in the adjacent elements, the modulus of the defect element for case 7 was set equal to 0.001 psi. The result of the analysis shows that the stress in the defect element is equal to 0.933 psi (case 8 in Fig.8). This indicates that in order to simulate a void, the modulus of the defect element should be set equal to or less than 0.001 psi.

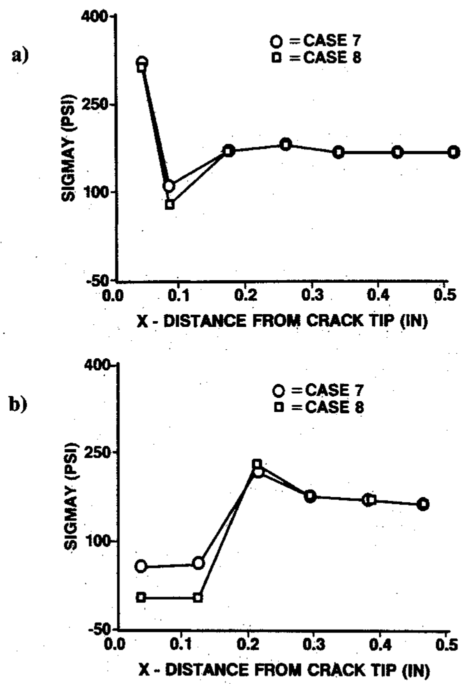

Fig. 8 Normal stress distribution at $Z = 0.15$ in. (case 8): a) along crack plane; and b) along defect plane.

The result of the analysis also shows that, by setting the modulus of the defect element equal to 0.001 psi, only the stresses in the defect elements and the adjacent elements are affected. By comparing case 8 with case 7, in the same layer, the stress in the element directly above the defect element is reduced from 121 to 99.2 psi whereas the stress in the element adjacent to the right side (in the positive x direction) of the defect element is increased from 220 to 230 psi as shown in Fig. 8. It is interesting to point out that, for the two cases considered (7 and 8) in this study, the presence of a void produces a negligible effect on the magnitude and distribution of K_I along the crack front as shown in Table 1.

IV. Conclusions

In this study, a three-dimensional elastic analysis of crack-defect interaction was conducted using finite element methods. The results of the finite element analysis reveal that, depending on the size and the location of the defect, the presence of a defect can change the magnitude and distribution of stress intensity factor along the crack front and can significantly affect the stress distribution in the defect-affected zone. The size of the defect-affected zone depends on the thickness of the defect; the larger the thickness the larger the defect-affected zone size. The result of the analysis also reveals that, in order to simulate a void, the modulus of the defect element should be set equal to or less than 0.001 psi. For the two cases (7 and 8) considered, the presence of a void affects only the stresses in the adjacent elements and produces a negligible effect on the magnitude and the distribution of K_I along the crack front.

Acknowledgments

The work was supported by the Office of Scientific Research, Air Force Systems Command. The author expresses his appreciation to C. W. Smith of Virginia Polytechnic Institute and State University for his helpful discussion, and to G. Langberg and R. Hansen for their assistance.

References

[1]Rubinstein, A. A., "Macrocrack-Microcrack Interaction," American Society of Mechanical Engineers, Paper No. 86-WA-APM-19, Anaheim, CA, Dec. 1986.

[2]Rossmanith, H. P., "Modeling of Fracture Process Zones and Singularity Dominated Zones," *Engineering Fracture Mechanics*, Vol. 17, No. 6, 1983, pp 509–526.

[3]Chudnovsky, A., and Moet, A., "Effect of Damage Dissemination on Crack Propagation in Polypropylene," *Journal of Applied Physics*, Vol. 54, No. 10, 1983, pp. 5562–5567.

[4]Liu, C. T., "Numerical Modeling of Crack-Defect Interaction—Part I," AIAA Paper 89-2646, July 1989.

[5]Liu, C. T., "Numerical Modeling of Crack-Defect Interaction—Part II," Seventh International Conference on Mathematical and Computer Modeling, Chicago, IL, Aug. 2–5, 1989.

[6]Kathiresan, K., and Atluri, S. N., "Three-Dimensional Homogeneous and *B*-Material Fracture Analysis for Solid Rocket Motor Grains by a Hybrid Displacement Finite Element Method," Georgia Inst. of Technology, AFRPL-TR-78-65, Atlanta, GA, April 1978.

[7]Liu, C. T., Jacobsen, A. E., and Thrasher, D. I., "Effect of Poisson's Ratio on Stress Intensity Factors," 1982 JANNAF Structures and Mechanical Behavior Meeting, Chemical Propulsion Information Agency, Applied Physics Lab., CPIA Pub. 368, Laurel, MD, Oct. 1982, pp. 379–390.

[8]Theiss, T. J., "Preliminary Investigation into the Cracking of Polyurethane," Master's Thesis, Virginia Polytechnic Inst. and State Univ., Blacksburg, VA, 1987.

[9]Post, D., Smith, C. W., and Czarnek, R., "Crack Opening and Extension in Inert Solid Propellant," Virginia Polytechnic Inst. and State Univ., AFAL-TR-87-043, Blacksburg, VA, March 1987.

[10]Post, D., Smith, C. W., and Czarnek, R., "Boundary Layer and Singularity Measurement in Three-Dimensional Fracture Problems," Virginia Polytechnic Inst. and State Univ., AFAL-TR-88-086, Blacksburg, VA, Oct. 1988.

Earl A. Thornton
Associate Editor